

Dynamic localization versus photon-assisted transport in semiconductor superlattices driven by dc-ac fields

W.-X. Yan

*Institute of Theoretical Physics, Shanxi University, Taiyuan, 030006, China
and China Center of Advanced Science and Technology (World Laboratory), P.O. Box 8730, Beijing 100080, China*

S.-Q. Bao and X.-G. Zhao

Institute of Applied Physics and Computational Mathematics, P.O. Box 8009, Beijing 100088, China

J.-Q. Liang

*Institute of Theoretical Physics, Shanxi University, Taiyuan, 030006, China
and China Center of Advanced Science and Technology (World Laboratory), P.O. Box 8730, Beijing 100080, China
(Received 22 December 1997)*

Via the numerical analysis on the intraband dynamics of optically excited semiconductor superlattices, it is found that time-integrated squared THz emission signals can be used for probing both dynamic localization and multiphoton resonance in the coherent regime. Competition effect between dynamic localization and photon-assisted transport has also been discussed.

Recently, semiconductor superlattice (SL) driven by external electric fields has been a subject of intensive investigations both theoretically and experimentally. The most significant example is Bloch oscillation (BO), which was theoretically predicted many years ago and experimentally demonstrated recently in SL driven by a uniform electric field. Within the tight-binding approximation, an intense laser field (ac fields) can make a charged particle localized around the initially injected place, which is the so-called dynamic localization.¹ Then the natural subsequent question will be the following: What will happen if the electrons in SL are subject to the combined dc-ac fields? Actually, this question is answered by the recent several theoretical predictions and experimental observations. For example, multiphoton absorption,² absolute negative conductivity,³ photon-assisted transport,⁴ fractional Wannier-Stark ladders,⁵ dynamic delocalization,⁶ excitonic Bloch oscillations⁷ etc. Particularly, the recent experiment on the multiple quantum-well superlattices driven by dc-ac fields has confirmed through probing the static I - V characteristics that the electrons in SL can tunnel through the adjacent wells through the stimulated emission and absorption of photons.⁴ In this facet, the common action of the dc-ac field plays the constructive role on the transport properties in SL. However, the dc-ac field can also play the destructive role on the transport in SL, which can be manifested in dynamic localization induced by dc-ac fields, provided that the ratio of the Stark frequency $\omega_B (= eF_0d)$, d is the SL lattice constant and F_0 is the amplitude of dc fields) to the ac field frequency ω is an integer n , and $edF_1/\hbar\omega$ (F_1 is the amplitude of ac fields) is a root of ordinary Bessel function of the order n : $J_n(edF_1/\hbar\omega) = 0$.¹ In this case, the electrons will become localized. Hence, the effects from both dc and ac fields play the dual role in the transport properties in SL.

In the static regime, the usual method in the investigation of transport properties in SL under the influence of external fields is through the observation of static I - V characteristics.⁴

In the realm of ultrashort laser pulse (usually in hundreds of femtosecond duration) generated coherent regime, what physical quantity can be used to probe the transport properties induced by the pure ac fields? This question was answered in detail by T. Meier *et al.* with the help of the well-known semiconductor Bloch equations.^{8,9} They found by monitoring the time-integrated squared THz emission signals that even in the presence of excitonic interactions comparable to the miniband widths, the carriers driven by pure intense laser fields (ac fields) reveal dynamic localization provided that $edF_1/\hbar\omega$ coincides with the roots of the ordinary Bessel function of order zero.^{1,9} Inspired by their work, we, in this report, show by numerical simulations that in the dc-ac fields, the detection of time-integrated squared THz signals not only can be used to probe the dc-ac-induced dynamic localization but also be employed to probe the photon-assisted transport in the presence of excitonic interactions in the coherent regime.

We begin with the following semiconductor Bloch equations by including the longitudinal external driving fields $\mathbf{F}(t)$ ^{8,9}

$$\begin{aligned} & \left[\frac{\partial}{\partial t} - \frac{e}{\hbar} \mathbf{F}(t) \cdot \nabla_{\mathbf{k}} - \frac{i}{\hbar} [e_c(\mathbf{k}, t) - e_v(\mathbf{k}, t)] \right] P(\mathbf{k}, t) \\ & = \frac{i}{\hbar} [n_c(\mathbf{k}, t) - n_v(\mathbf{k}, t)] \Omega(\mathbf{k}, t) + \left. \frac{\partial P(\mathbf{k}, t)}{\partial t} \right|_{\text{coll}}, \end{aligned} \quad (1)$$

$$\begin{aligned} & \left[\frac{\partial}{\partial t} - \frac{e}{\hbar} \mathbf{F}(t) \cdot \nabla_{\mathbf{k}} \right] n_{c,(v)}(\mathbf{k}, t) = \mp \frac{2}{\hbar} \text{Im}[\Omega(\mathbf{k}, t) P^*(\mathbf{k}, t)] \\ & + \left. \frac{\partial n_{c,(v)}(\mathbf{k}, t)}{\partial t} \right|_{\text{coll}}. \end{aligned} \quad (2)$$

In the above equations, $n_c(\mathbf{k}, t)$ and $n_v(\mathbf{k}, t)$ are the populations in the conduction and valence bands, respectively. $P(\mathbf{k}, t)$ is the interband polarization. $e_{c,(v)}(\mathbf{k}, t) = \epsilon_{c,(v)}(\mathbf{k}, t) - \sum_{\mathbf{k}'} V(\mathbf{k}, \mathbf{k}') n_{c,(v)}(\mathbf{k}', t)$ are the electron and hole energies by taking into account the excitonic interaction, while, $\epsilon_{c,(v)}(\mathbf{k}, t)$ are the corresponding energies of the conduction and (valence) bands with no Coulomb interaction. $\Omega(\mathbf{k}, t) = \mu E(t) + \sum_{\mathbf{k}'} V(\mathbf{k}, \mathbf{k}') P(\mathbf{k}', t)$ is the renormalized Rabi frequency and $V(\mathbf{k}, \mathbf{k}')$ is the Coulomb potential in the quasimomentum space. $E(t)$ is the optical field and assumed to be the Gaussian laser pulses.^{8,9} $\mathbf{F}(t)$ is the combined dc-ac fields: $\mathbf{F}(t) = \mathbf{F}_0 + \mathbf{F}_1 \cos(\omega t)$. Incoherent dissipative processes are phenomenologically described by the last terms in Eqs. (1) and (2).

If the strength of the optical field $E(t)$ is weak, the low excitation regime can be produced. In this regime, the perturbation expansion of Eqs. (1) and (2) in terms of the optical field can be performed by the following procedure:^{8,10} $n_{c,(v)}(\mathbf{k}, t) = n_{c,(v)}^{(0)}(\mathbf{k}, t) + n_{c,(v)}^{(2)}(\mathbf{k}, t) + \dots$; $P(\mathbf{k}, t) = P^{(1)}(\mathbf{k}, t) + P^{(3)}(\mathbf{k}, t) + \dots$. The usual initial condition that electron dwell on the valence band before being excited is adopted.

For simplicity, we focus on the one-dimensional case, which is just the SL growth direction (assumed to be z direction). Although we build our model on a simple one-dimensional system, the contribution from the other two directions (in \mathbf{k} space) which is perpendicular to the longitudinal electric field can be treated as inhomogeneous broadening.¹¹ This broadening does not influence the profile of the THz signal qualitatively.¹² Another aspect for the reasonability of this model can be found in Refs. 6 and 7. The driving dc-ac field is also assumed to be along the growth direction, and we adopt the contact Coulomb potential $V\delta(z-z')$, which carries the most important excitonic characteristics.¹³ Under the above assumptions, the partial differential equations for the first order $P^{(1)}(k, t)$ and the second order $n^{(2)}(k, t)$ ⁸ can be reduced to the following integrodifferential equations with the help of the accelerated basis in the quasimomentum k : [by changing k to $k - \eta(t)$, and $\eta(t)$ is defined as: $\eta(t) = e/\hbar \int_0^t F(t') dt'$] (Ref. 14)

$$\begin{aligned} & \left\{ \frac{\partial}{\partial t} - \frac{i}{\hbar} [\epsilon_c(k - \eta(t), t) - \epsilon_v(k - \eta(t), t) + V] \right\} \tilde{P}^{(1)}(k, t) \\ &= -\frac{i}{\hbar} \left[\mu E(t) + V \sum_q \tilde{P}^{(1)}(q, t) \right] - \frac{\tilde{P}^{(1)}(k, t)}{T_2}, \quad (3) \\ & \frac{\partial \tilde{n}_{c,(v)}^{(2)}(k, t)}{\partial t} = \mp \frac{2}{\hbar} \text{Im} \left\{ \left[\mu E(t) + V \sum_q \tilde{P}^{(1)}(q, t) \right] \right. \\ & \quad \left. \times \tilde{P}^{(1)*}(k, t) \right\} - \frac{\tilde{n}_{c,(v)}^{(2)}(k, t)}{T_1}, \quad (4) \end{aligned}$$

where we have introduced the following new notations for convenience:

$$\begin{aligned} \tilde{P}^{(1)}(k, t) &= P^{(1)}[k - \eta(t), t], \\ \tilde{n}_{c,(v)}^{(2)}(k, t) &= n_{c,(v)}^{(2)}[k - \eta(t), t]. \end{aligned} \quad (5)$$

In Eqs. (3) and (4), we adopt the relaxation approximation by introducing the longitudinal time T_1 and transverse relaxation time T_2 , respectively, to replace the collision terms. The treatment of these terms beyond the relaxation approximation can be realized by several ways, for example, direct integration of the equations of motion,¹⁵ Monte Carlo simulation,¹⁶ etc.

As mentioned previously, what we want to do is to calculate the time-integrated squared THz signal. The THz emission signal in SL can be expressed as $S_{\text{THz}}(t) \propto \partial_t j^{(2)}(t)$, where $j^{(2)}(t) = e/\hbar \sum_i \int \partial \epsilon_i(k) / \partial k n_i^{(2)}(k, t) dk$ ($i = c, v$) is the current due to the nonequilibrium distribution of electrons and holes excited by the Gaussian laser pulses. This current can be rewritten in the following equivalent form with the help of accelerated basis

$$j^{(2)}(t) = \frac{e}{\hbar} \sum_i \int \frac{\partial \epsilon_i[k - \eta(t)]}{\partial k} \tilde{n}_i^{(2)}(k, t) dk \quad (i = c, v). \quad (6)$$

Solving Eqs. (3) and (4) in the accelerated basis in k space is more convenient than the direct integration in the usual quasimomentum space. In the following numerical simulation, we use the similar parameters as those used by T. Meier *et al.* The combined miniband width $\Delta = \Delta_c + \Delta_v = 20$ meV (here, we use the tight-binding model as in Ref. 9); Coulomb potential strength $V = 10$ meV. The central frequency of the optical field is assumed to be located at 2 meV below excitonic resonance. The full width at half maximum of Gaussian laser pulse envelope $|E(t)|^2$ is chosen to be 100 fs.¹⁷ Both longitudinal T_1 and transverse relaxation time T_2 have been set to be 2 ps. The energy quantum of the ac field $\hbar \omega$ is fixed to be 20 meV. To capture the information on dynamic localization, we set the ratio of the Stark frequency ω_B to the ac field frequency ω to be an integer, e.g., $n = 1$, without loss of generality. We change the ratio $eF_1 d / \hbar \omega$ continuously, and monitor the time-integrated squared THz emission signal through the calculation of the following quantity:

$$T_s \propto \int d\tau |S_{\text{THz}}(\tau)|^2. \quad (7)$$

The plot of the time-integrated THz signal vs the ratio $eF_1 d / \hbar \omega$ has been shown in Fig. 1. In this figure, it can be clearly seen that when the ratio $eF_1 d / \hbar \omega$ scans through 3.95, 6.95, 10.0, which are approximately the roots of the ordinary Bessel function of the first order J_1 , the time-integrated squared signal falls into valleys. While the peaks in the plot lie in the vicinity at those values of $eF_1 d / \hbar \omega$ that make $|J_1(eF_1 d / \hbar \omega)|^2$ reach the local maxima. From the above effect, it is obvious that $|J_1(eF_1 d / \hbar \omega)|^2$ reflects the signal T_s profile qualitatively. All the above phenomena demonstrate that even in the presence of Coulomb excitonic interaction whose strength is comparable to the miniband widths of SL, dc-ac induced dynamic localization still appears. This kind of dynamic localization can be probed through the observation of the signal T_s just like the case of a pure ac field.⁹

Another aspect of the combined dc-ac fields on the transport of the SL lies in that electrons/holes can tunnel through

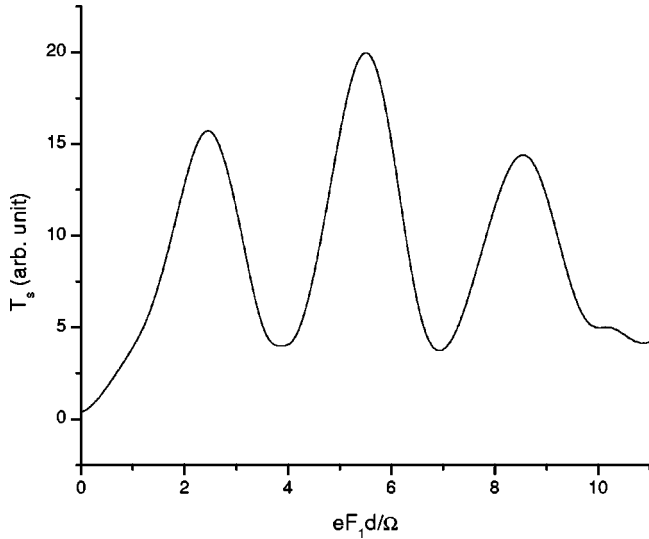


FIG. 1. The plot of time-integrated squared THz emission signal vs the ratio $eF_1 d / \Omega (\Omega = \hbar \omega)$, showing the dynamic localization induced by dc-ac fields. The parameters used in this figure are declared in the text.

the adjacent wells through the photon emission and absorption, when the ratio of the Stark frequency of dc field ω_B to the ac field frequency ω is an integer.³ This phenomenon is the so-called *inverse Bloch oscillators*, which was found in a recent experimental study by Unterrainer *et al.* in the static regime.⁴ The coherent regime counterpart of this effect can also be found in our numerical calculation, which was shown in Fig. 2. In this figure, we give the plot of the time-integrated squared THz emission signal vs the ratio ω_B / ω , and set the ratio $eF_1 d / \hbar \omega$ to be 2.0. From the figure, we can see that the large peaks appear at the location where the ratio ω_B / ω is an integer. The other distinctive peaks, which appear at fractional ω_B / ω can be attributed to the dynamical

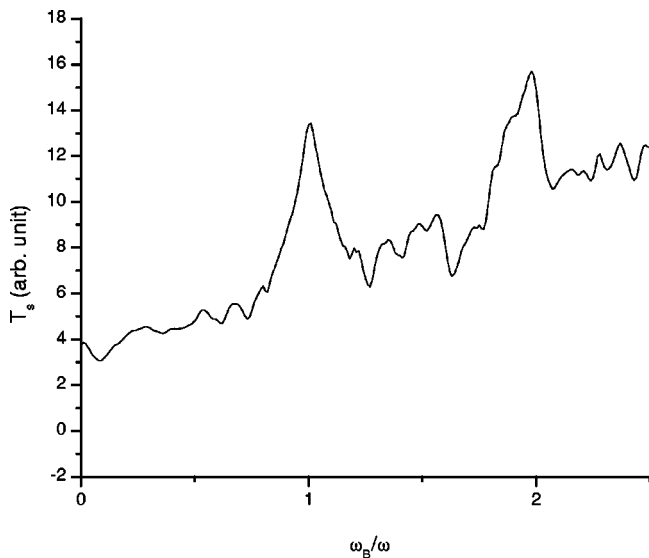


FIG. 2. The plot of time-integrated squared THz emission signal vs the ratio ω_B / ω , multiphoton resonance can be clearly seen. We choose the ratio $eF_1 d / \hbar \omega$ to be 2.0, which is well away from the roots of the first-order ordinary Bessel function.

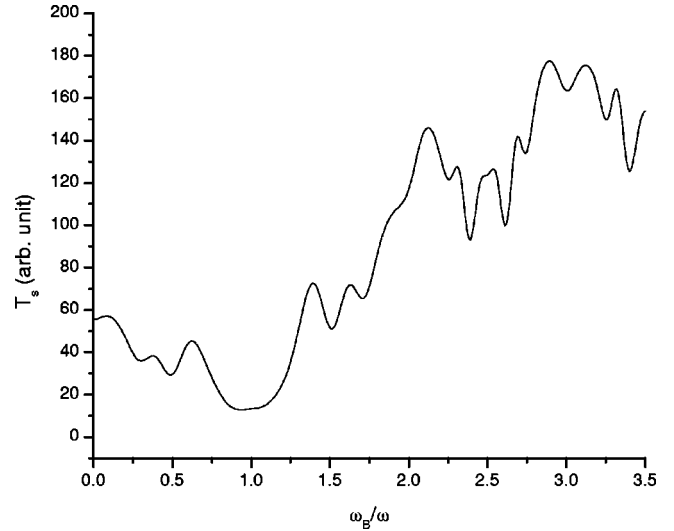


FIG. 3. The same plot as that of Fig. 2, but we choose the ratio $eF_1 d / \Omega (\Omega = \hbar \omega)$ to be 3.8, which is around the root of the first-order ordinary Bessel functions.

fractional Wannier-Stark ladders theoretically proposed recently.^{5,6,18}

Let us look at the competition effect between the dc-ac-induced dynamic localization and the photon-assisted transport facilitated by coupling of the combined dc-ac fields. The competition between these two effects is shown in Fig. 3, where the plot of the time-integrated squared THz emission signals vs the ratio ω_B / ω is given. In this figure, we set the ratio $eF_1 d / \hbar \omega$ to be 3.8, which is around the first root of the ordinary Bessel function of the first order. It can be clearly seen that the signal shows a deep valley when the ratio ω_B / ω reaches around the unity. While, the peaks appearing at $\omega_B / \omega = 2, 3$ are still present. In other words, the one-photon-assisted transport has been suppressed by this specific selection of field parameters, and the dynamic localization prevails over the one-photon-assisted transport. If we shift the ratio from those values that are in the vicinity of the roots of the first-order ordinary Bessel function, the one-photon-assisted transport can revive. This regeneration can be clearly seen from Fig. 2. We can further suppress the two-photon resonance by selecting the ratio ω_B / ω to be 2, and another ratio $eF_1 d / \hbar \omega$ to be the roots of the ordinary Bessel function of the order 2, i.e., make $J_2(eF_1 d / \hbar \omega) = 0$, which we do not show for saving space.

In summary, using the tight-binding model driven by dc-ac fields and perturbatively solving the semiconductor Bloch equations in the accelerated quasimomentum space, we found that the time-integrated squared THz emission signal reveals both the dynamic localization and the multiphoton resonance in the coherent regime. The dynamic localization can be fulfilled when the ratio of Stark frequency ω_B of dc fields to the ac field frequency ω is an integer n , and the another ratio $eF_1 d / \hbar \omega$ is located around one of the roots of the n th order ordinary Bessel function J_n . The dynamic localization is embodied by suppressing the oscillation amplitude of the THz emission signals. Multiphoton assisted transport (resonance) can be identified when time-integrated

squared THz emission signals reach peaks provided that the ratio ω_B/ω is an integer, and another ratio $eF_1d/\hbar\omega$ is not in the vicinity of the roots of the ordinary Bessel function of integral order. Otherwise, the photon-assisted transport will be destroyed by the dynamic localization. Experimentally, one can choose GaAs/Al_{0.3}Ga_{0.7}*p-i-n* superlattices with well width 95 angstroms and thin barrier (about 25 angstroms) (Ref. 19) biased by both dc and intense free electron laser (ac field) along the lattice growth direction and excited by optical pulses to be the realistic system. This choice is believed to be able to produce the desired parameters declared in the text. Adjusting the parameters $edF_1/\hbar\omega$, ω_B/ω , as de-

scribed in the text accordingly, the theoretical findings in our text should be revealed. The experimental arrangements can be prepared in a similar way as those used by UCSB group.^{3,4}

The authors thank Dr. T. Meier for stimulating and useful discussions. This work was supported in part by the National Natural Science Foundations of China under Grant No. 19724517, a grant of China Academy of Engineering and Physics, and China Postdoctoral Science Foundation; also grants from Shanxi University Research Foundations; Youth Science Foundation of Shanxi province.

-
- ¹D. H. Dunlap and V. M. Kenkre, Phys. Rev. B **34**, 3625 (1986); M. Holthaus, Phys. Rev. Lett. **69**, 351 (1992); A. W. Ghosh, A. V. Kuznetsov, and J. W. Wilkins, *ibid.* **79**, 3494 (1997).
- ²B. S. Monozon, J. L. Dunn, and C. A. Bates, Phys. Rev. B **50**, 17 097 (1994); J. Phys.: Condens. Matter **8**, 877 (1996).
- ³B. J. Keay, S. Zeuner, S. J. Allen, Jr., K. D. Maranowski, A. C. Gossard, U. Bhattacharya, and M. J. W. Rodwell, Phys. Rev. Lett. **75**, 4102 (1995).
- ⁴K. Unterrainer, B. J. Keay, M. C. Wanke, S. J. Allen, D. Leonard, G. Medeiros-Ribeiro, U. Bhattacharya, and M. J. Rodwell, Phys. Rev. Lett. **76**, 2973 (1996).
- ⁵X.-G. Zhao, R. Jahnke, and Q. Niu, Phys. Lett. A **202**, 297 (1995); X.-G. Zhao, G. A. Georgakis, and Q. Niu, Phys. Rev. B **56**, 3976 (1997).
- ⁶Ren-Bao Liu and Bang-Fen Zhu, Phys. Rev. B **59**, 5759 (1999).
- ⁷M. M. Dignam, Phys. Rev. B **59**, 5770 (1999); M. M. Dignam, J. E. Sipe, and J. Shah, *ibid.* **49**, 10 502 (1994).
- ⁸For a general review about semiconductor Bloch equations, see H. Haug and S. W. Koch, *Quantum Theory of the Optical and Electronic Properties of Semiconductors*, 3rd ed. (World Scientific, Singapore, 1994); the cases including the external electric field can be found in T. Meier, G. von Plessen, and P. Thomas, Phys. Rev. Lett. **73**, 902 (1994).
- ⁹T. Meier, G. von Plessen, and P. Thomas, Phys. Rev. B **51**, 14 490 (1995).
- ¹⁰Y. R. Shen, *The Principles of Nonlinear Optics* (Wiley, New York, 1984), p. 9.
- ¹¹G. von Plessen and P. Thomas, Phys. Rev. B **45**, 9185 (1992).
- ¹²For dc case, one can see this by comparing Fig. 3 of Ref. 8 with Fig. 4 of Ref. 9.
- ¹³S. Schmitt-Rink, D. S. Chemla, W. H. Knox, and D. A. B. Miller, Opt. Lett. **15**, 60 (1990).
- ¹⁴W. Quade, E. Schöll, F. Rossi, and C. Jacoboni, Phys. Rev. B **50**, 7389 (1994).
- ¹⁵J. Hader, T. Meier, S. W. Koch, F. Rossi, and N. Linder, Phys. Rev. B **55**, 13 799 (1997).
- ¹⁶T. Kuhn and F. Rossi, Phys. Rev. Lett. **69**, 977 (1992); T. Meier, F. Rossi, P. Thomas, and S. W. Koch, *ibid.* **75**, 2558 (1995).
- ¹⁷In time-resolved signals, the profile of THz signal depend sensitively on the excitation conditions, while in time-integrated cases, it is qualitatively insensitive.
- ¹⁸Q. Niu, X.-G. Zhao, G. A. Georgakis, and M. G. Raizen, Phys. Rev. Lett. **76**, 4504 (1996).
- ¹⁹A. M. Fox, D. A. B. Miller, J. E. Cunningham, W. Y. Jan, C. Y. P. Chao, and C. L. Chuang, Phys. Rev. B **46**, 15 365 (1992).